

1-1-2011

## Star clusters in M31: Old clusters with bar kinematics

H. Morrison  
*Case Western Reserve University*

N. Caldwell  
*Center for Astrophysics*

R. P. Schiavon  
*Gemini Observatory*

E. Athanassoula  
*LAM/OAMP*

Aaron J. Romanowsky  
*San Jose State University, aaron.romanowsky@sjsu.edu*

*See next page for additional authors*

Follow this and additional works at: [https://scholarworks.sjsu.edu/physics\\_astron\\_pub](https://scholarworks.sjsu.edu/physics_astron_pub)



Part of the [Astrophysics and Astronomy Commons](#)

---

### Recommended Citation

H. Morrison, N. Caldwell, R. P. Schiavon, E. Athanassoula, Aaron J. Romanowsky, and P. Harding. "Star clusters in M31: Old clusters with bar kinematics" *Astrophysical Journal Letters* (2011). <https://doi.org/10.1088/2041-8205/726/1/L9>

This Article is brought to you for free and open access by the Physics and Astronomy at SJSU ScholarWorks. It has been accepted for inclusion in Faculty Publications by an authorized administrator of SJSU ScholarWorks. For more information, please contact [scholarworks@sjsu.edu](mailto:scholarworks@sjsu.edu).

---

**Authors**

H. Morrison, N. Caldwell, R. P. Schiavon, E. Athanassoula, Aaron J. Romanowsky, and P. Harding

## STAR CLUSTERS IN M31: OLD CLUSTERS WITH BAR KINEMATICS

HEATHER MORRISON<sup>1</sup>, NELSON CALDWELL<sup>2</sup>, RICARDO P. SCHIAVON<sup>3</sup>, E. ATHANASSOULA<sup>4</sup>,  
AARON J. ROMANOWSKY<sup>5</sup>, AND PAUL HARDING<sup>1</sup>

<sup>1</sup> Department of Astronomy, Case Western Reserve University, Cleveland, OH 44106-7215, USA; [heather@vegemite.case.edu](mailto:heather@vegemite.case.edu), [paul.harding@case.edu](mailto:paul.harding@case.edu)

<sup>2</sup> Center for Astrophysics, 60 Garden Street, Cambridge, MA 02138, USA; [caldwell@cfa.harvard.edu](mailto:caldwell@cfa.harvard.edu)

<sup>3</sup> Gemini Observatory, 670 N. A'ohoku Place, Hilo, HI 96720, USA; [rschiavo@gemini.edu](mailto:rschiavo@gemini.edu)

<sup>4</sup> LAM/OAMP, UMR6110, CNRS/Univ. de Provence, 38 rue Joliot Curie, 13388 Marseille 13, France; [lia@oamp.fr](mailto:lia@oamp.fr)

<sup>5</sup> UCO/Lick Observatory, University of California, Santa Cruz, CA 95064, USA; [romanow@ucolick.org](mailto:romanow@ucolick.org)

Received 2010 October 5; accepted 2010 November 10; published 2010 December 13

### ABSTRACT

We analyze our accurate kinematical data for the old clusters in the inner regions of M31. These velocities are based on high signal-to-noise Hectospec data. The data are well suited for analysis of M31's inner regions because we took particular care to correct for contamination by unresolved field stars from the disk and bulge in the fibers. The metal-poor clusters show kinematics that are compatible with a pressure-supported spheroid. The kinematics of metal-rich clusters, however, argue for a disk population. In particular the innermost region (inside 2 kpc) shows the kinematics of the  $x_2$  family of bar periodic orbits, arguing for the existence of an inner Lindblad resonance in M31.

*Key words:* galaxies: individual (M31) – galaxies: kinematics and dynamics – galaxies: star clusters: general – galaxies: star clusters: individual – globular clusters: general

### 1. INTRODUCTION

Globular clusters can provide simultaneous estimates of velocity, metallicity, and age: a powerful trio with which to study the history of a galaxy. They are particularly helpful to complement integrated light studies, which average over all stellar populations along a line of sight. In this Letter, we discuss the kinematics of old clusters projected on the inner 10 kpc of M31. Roughly one-third of our sample of over 300 old clusters in M31 (presented in Caldwell et al. 2009, 2010, Papers I and II hereafter) are located within 3 kpc of its center. Because of our careful treatment of the effect of field star contamination from the bright bulge and inner disk region in our fibers, our data set is particularly well suited for study of the central regions of M31.

Early work on bulge kinematics (Davies et al. 1983) showed that bulges resemble low-luminosity ellipticals in being kinematically hot with a high degree of rotational support ( $V/\sigma \sim 1$ ). Later studies, however, showed that bulges are more complex and that an important distinction must be made between classical  $R^{1/4}$  bulges—which are kinematically hot and formed rapidly from mergers and collapses—and bulges formed via secular evolution of disks, which have a lower Sérsic index (Kormendy & Kennicutt 2004). In this second category Athanassoula (2005) distinguished the boxy/peanut bulges—which are parts of bars seen edge-on—and the disk-like bulges, which have a disk shape. Boxy/peanut bulges can be distinguished in near-edge-on galaxies from photometry or via kinematics (e.g., Kuijken & Merrifield 1995; Bureau & Athanassoula 1999).

Evidence from isophotal twists and kinematics was used to argue that M31 might have a triaxial bulge or a bar (Lindblad 1956; Stark 1977; Stark & Binney 1994). More recently, Athanassoula & Beaton (2006) and Beaton et al. (2007), using deep Two Micron All Sky Survey (2MASS) observations, considerably strengthened the case for a bar and suggested that M31 also has a centrally concentrated classical bulge, which dominates the light in the inner 200 pc. We note here that this is a considerably smaller and less dominant classical bulge than

the one suggested by previous authors: de Vaucouleurs (1958) found an effective radius of 3.5 kpc, and Walterbos & Kennicutt (1988) derived an effective radius of 2 kpc and found that the bulge contributed 40% of the light of the galaxy. Our globular cluster kinematical data allow us to further explore this shift in our view of M31's bulge, since we have [Fe/H] and velocity measurements for 98 old clusters projected within 3 kpc of M31's center.

We assume a distance of 770 kpc throughout (Freedman & Madore 1990) and a P.A. of  $37^\circ:7$ . The  $XY$  coordinate system we use in this Letter has units of kpc, with positive  $X$  along the major axis toward the NE.

### 2. CLUSTER KINEMATICS

Paper II presented [Fe/H], age and velocity measurements based on high signal-to-noise (S/N) Hectospec (Fabricant et al. 2005) spectra (a median S/N of 75 per Å) for over 300 M31 clusters with ages greater than 6 Gyr. (In fact the great majority of these clusters have ages greater than 10 Gyr.) Here we discuss the old clusters from Paper II which are within 2 kpc of M31's major axis. Repeat Hectospec observations showed a median velocity error of  $6 \text{ km s}^{-1}$ . Our study contains 17 entirely new cluster velocities and is the first fiber study to use offset exposures near each cluster in the bright inner regions to correct for the contamination from field stars there. Caldwell et al. (2010) showed that ignoring this effect can lead to velocity errors of more than  $100 \text{ km s}^{-1}$ . In the small number of cases where our velocities differed significantly from the Hectochelle velocities of J. Strader & N. Caldwell (2011, in preparation), we have used the more accurate Hectochelle data. Our [Fe/H] values are in good agreement with the recent results of Beasley et al. (2005) and Colucci et al. (2009) and the *Hubble Space Telescope* (HST) color–magnitude derived values. We found that the old cluster metallicity distribution was neither unimodal nor simply bimodal, showing a median [Fe/H] around  $-1.0$  and possible peaks at [Fe/H] =  $-0.3$ ,  $-0.8$ , and  $-1.4$ .

Previous work on M31 globulars suggested a larger systemic rotation for the metal-richer clusters (e.g., Huchra et al. 1991;

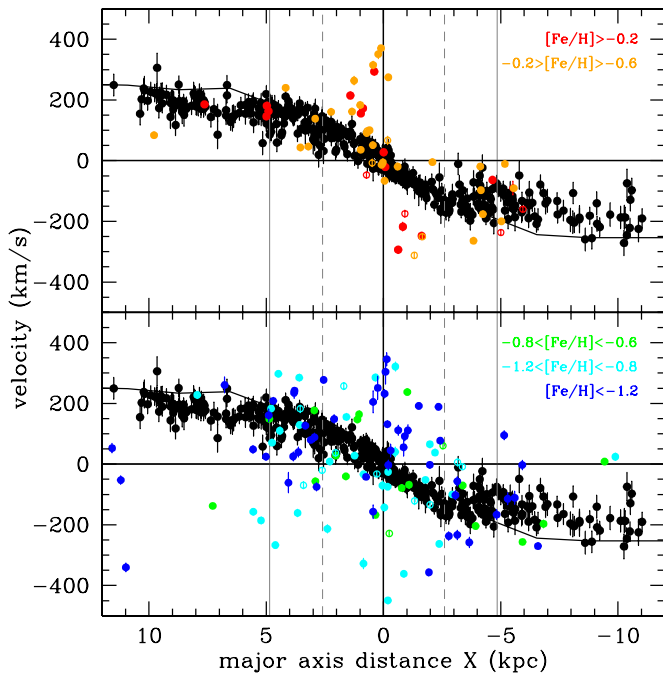


**Figure 1.** Velocity of clusters projected less than 2 kpc from the major axis. The upper panel shows the metal-rich clusters ( $[\text{Fe}/\text{H}] > -0.6$ ) and the lower panel the more metal-poor clusters which dominate M31’s old clusters. In both panels, black symbols show the *mean* velocity of stars at that position, integrated along the line of sight. Open symbols denote ages less than 10 Gyr, closed symbols greater than 10 Gyr (note that we are unable to measure ages for clusters with  $[\text{Fe}/\text{H}]$  less than  $-1.0$ , and we use closed symbols for these clusters). The vertical gray lines show the end of the thick bar (dashed lines) and the thin bar (solid), from Beaton et al. (2007) and Athanassoula & Beaton (2006), and the solid black line is the rotation curve from Kent (1989). Note that measurements of the dimensions of the thin and particularly the thick bar are approximate only.

Barmby et al. 2000). Since all but one of the clusters with  $[\text{Fe}/\text{H}] > -0.4$  are projected on the inner disk (less than 1.5 kpc from the major axis) we first explore connections between the metal-rich clusters and M31’s disk. In the Milky Way, the metal-rich globular clusters are likely associated with its inner disk: Zinn (1985) connected these clusters with the thick disk and Minniti et al. (1996) with the bulge. Since more recent work has shown that the Milky Way bulge is dominated by a bar (Weiland et al. 1994; Binney et al. 1997), the most metal-rich globulars in the Milky Way are all likely to be connected to its disk in some way: either as a bar distortion or a thicker component.

To compare our old clusters with M31’s disk, we use the fibers which were designed to measure the contamination from M31’s disk and bulge: each fiber’s measured velocity will be the *mean* velocity of all the stars along that line of sight. Figure 1 compares cluster velocities (with different colors for clusters with different metallicities: red for most metal rich though blue for the most metal poor) with these mean velocity estimates, shown in black. The top panel shows clusters with  $[\text{Fe}/\text{H}] > -0.6$ ; the bottom panel shows more metal-poor clusters. The difference between their kinematic behavior is stunning.

Metal-poor clusters (lower panel) show little sign of rotation and occupy the four quadrants of the plot similarly. On the other hand, the metal-rich clusters (upper panel) show a distinct and quite cold kinematical signature. There are almost no clusters in the forbidden quadrants (occupancy here corresponds to rotation in the opposite direction to the disk) and most of those more than 2 kpc from the center (i.e.,  $|X| > 2$ ) have velocities which closely follow the disk velocity at that position. However, in the inner 2 kpc the signature differs from the usual one for

a disk composed of stars on near-circular orbits. Although all except one cluster occupy the same quadrant as the disk, thus respecting the same direction of rotation, their velocities can deviate from the local mean velocity of the integrated light by up to  $350 \text{ km s}^{-1}$  (recall that M31’s rotation velocity is  $250 \text{ km s}^{-1}$ ). We note that very high velocities are also observed in the HI gas in this region (Brinks & Shane 1984). In the following section, we will describe expectations for the kinematics of thin disk, bar, and classical bulge objects, and show that this signature is expected for bar orbits.

### 2.1. Kinematics: Expectation from Disk, Bar, and Bulge

Thin disks in galaxies have “cold” kinematics dominated by rotation and show a low velocity dispersion. We showed in Paper I (see Figure 13) that the young M31 clusters (with ages less than 2 Gyr) have such kinematics: the young clusters all follow the same narrow locus in position versus velocity. We also showed (see Figure 12) the mean velocity field across the face of the disk, obtained from our “sky” fibers. The mean velocity changes smoothly and slowly as we look from the receding side of the disk through the center to the approaching side, as expected for a thin disk.

It is particularly simple to follow the kinematic signature of a cold, thin disk by examining velocities of objects seen close to the major axis. (This is why we have chosen to display only objects with  $|Y| < 2$ .) In a galaxy close to edge-on such as M31, such a star in a circular orbit will have all its velocity in the line of sight, giving a clean measure of  $V_\phi$ , the azimuthal component, from the line-of-sight velocity. For disk stars observed at larger distances from the major axis, less of their azimuthal velocity will be projected onto the line of sight and so the change in mean velocity from one side of the disk to the other will be smaller.

Most orbits in bars follow the two main families of closed periodic orbits (Binney & Tremaine 2008): the  $x_1$  orbits, which are aligned along the long axis of the bar (close to the major axis in M31; see Beaton et al. 2007), and  $x_2$  orbits which are aligned along its short axis (close to M31’s minor axis). For  $x_2$  orbits, velocities can reach very high values close to the center of the galaxy. This is due to the fact that they are observed near-end-on, so that the line-of-sight component is nearly along the orbit at its pericenter (Bureau & Athanassoula 1999). Figure 2 (from Binney et al. 1991) illustrates the spatial and velocity signatures of  $x_1$  and  $x_2$  orbits. It can be seen that in this example, the  $x_2$  orbits reach velocities much higher than the circular velocity. (A similar position–velocity diagram for an M31-like system can be seen in the middle top panel of Figure 11 of Athanassoula & Beaton 2006.)

Lastly, we would expect any classical bulge component to show  $V/\sigma \sim 1$ : some rotational support but a roughly equivalent amount of random motion. Kent (1989) fitted the M31 bulge using an oblate rotator model with major-axis velocity of around  $90 \text{ km s}^{-1}$  and velocity dispersion of  $130 \text{ km s}^{-1}$  at 1.5 kpc from the center.

## 3. DISCUSSION

We saw in Figure 1 that the kinematics of old M31 clusters with  $[\text{Fe}/\text{H}] > -0.6$  in its innermost region show the distinctive behavior of objects on  $x_2$  orbits in M31’s bar. This is in very good agreement with orbital structure in bars since the  $x_2$  orbits are always confined to the innermost regions, in the region interior to the inner Lindblad resonance (ILR). Most of the rest of the metal-rich clusters have orbits consistent with disk objects.

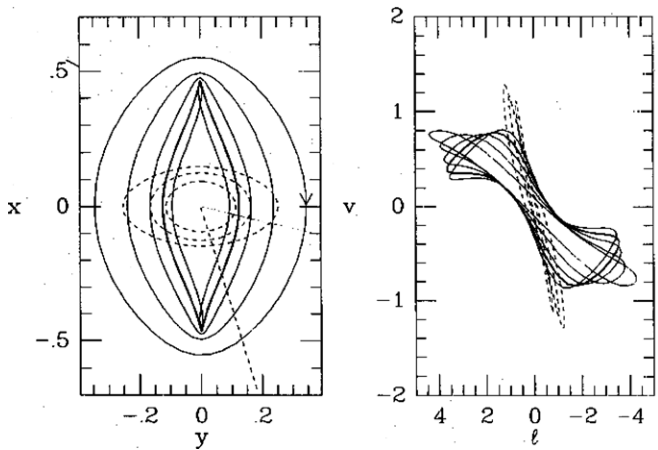


**Figure 2.** Illustration of regions occupied both spatially and kinematically by  $x_1$  and  $x_2$  orbits in a barred potential, from Binney et al. (1991). Left panel shows their spatial location in a face-on view, while the right panel shows longitude–velocity plots.  $x_1$  orbits are aligned along the bar major axis and shown with solid lines, while  $x_2$  orbits align perpendicular to the bar major axis and are shown with dotted lines. Note that in this example the  $x_2$  orbits can reach velocities significantly higher than the circular velocity, which is  $v = 1$  in this model.

We see little or no indication in the kinematics in the upper panel of Figure 1 for a kinematically hot population such as the classical bulge of Kent (1989). However, we note again that the classical bulge identified by Beaton et al. (2007) was quite small, only dominating the inner 200 pc. We have only one cluster within 200 pc of M31’s center in our sample, so we cannot probe the kinematics of this region in M31. Only in the lower panel, with the more metal-poor clusters, do we see a signature like that of a kinematically hot classical bulge: there are roughly equal numbers of clusters in each quadrant, and we see that the velocity dispersion rises sharply close to the center, as we would expect for a centrally concentrated classical bulge. However, as we shall show below, the starlight in this region is dominated by old metal-rich stars of near solar abundance, so these metal-poor clusters are not tracing the dominant component here.

To summarize, we see strong evidence from the kinematics of the metal-rich old clusters ( $[\text{Fe}/\text{H}] > -0.6$ ) for both disk and bar kinematics. A number of the clusters within 2 kpc of the center of M31 show the kinematic signature of  $x_2$  orbits in a barred potential. The rest of these clusters (plus the other metal-rich clusters within 2 kpc of the major axis) show the cold kinematics of the disk. These kinematics strongly confirm the result of Beaton et al. (2007) and Athanassoula & Beaton (2006) that M31 has a bar whose inner parts constitute the boxy bulge which dominates its light in the inner few kpc. To our knowledge, this is the first clear detection of globular clusters with bar kinematics in any galaxy. However, there is one massive cluster (the Arches cluster) in the Milky Way which has a large space velocity ( $232 \text{ km s}^{-1}$ ) and is currently at a projected distance of only 26 pc from the galactic center (Stolte et al. 2008). These authors note that the cluster could be on a transitional trajectory between  $x_1$  and  $x_2$  orbits in the Milky Way’s barred potential, and may have been formed in a starburst triggered when a massive molecular cloud “collided on the boundary between  $x_1$  and  $x_2$  orbits in the inner bar.”

### 3.1. Relations Between Clusters and Bulge/Disk Field Stars

We now consider the relationship between field stars and globular clusters in the inner regions of M31. Trager et al. (2000)

studied the integrated light of M31’s bulge, in a circular aperture of diameter 250 pc. They found a mean metallicity of +0.2 dex and a mean age of around 6 Gyr. More recently, Saglia et al. (2010) have made a detailed study of the M31 bulge region using a number of long-slit exposures with the Hobby Eberly Telescope. They find a mean metallicity around solar and an age of around 12 Gyr in the inner 1–2 kpc. (Note that they do see a metallicity gradient, reaching up to  $[\text{Z}/\text{H}] = +0.4$ , over the inner 200 pc, the region dominated by the classical bulge.)

Sarajedini & Jablonka (2005) used *HST*/WFPC2 observations to produce a color–magnitude diagram for M31’s bulge at 1.6 kpc from its center, and inferred a metallicity distribution which peaked near solar. Olsen et al. (2006) summarized near IR color–magnitude diagrams from high spatial resolution studies of M31 to find that the stellar population in the inner few kpc was dominated by old, nearly solar-metallicity stars. Interestingly, by comparing fields in the bulge with an inner disk field, they found no evidence for an age difference between bulge and disk. This is unsurprising if M31’s bulge is dominated by a bar, since bar stars are merely inner disk stars which have become part of the bar pattern.

The mean metallicity of the integrated light from field stars thus exceeds the mean metallicity of the globulars in the inner few kpc; it is closer to the mean of those with  $[\text{Fe}/\text{H}] > -0.6$ , which show either disk or bar kinematics. (It has been suggested before that globular clusters are formed less efficiently in metal-rich populations: Strader et al. (2005) calculate that the efficiencies differ by more than a factor of 10 in the Milky Way, by comparing metal-rich globular clusters to the bulge luminosity and metal-poor numbers to the halo luminosity. This number will not be changed radically if we substitute the thick disk luminosity for the bulge luminosity in this calculation.)

Thus, a simple picture can explain the existence of the metal-rich globular clusters in M31: they merely participated in the early formation of the inner disk and the onset of the bar instability.

## 4. SUMMARY

We have discussed accurate kinematical data for old M31 clusters in its inner regions within 2 kpc of its major axis. The majority of the metal-rich clusters (those with  $[\text{Fe}/\text{H}]$  greater than  $-0.6$ ) show disk kinematics, and many of the clusters within the innermost bar region have the signature of the  $x_2$  family. This clearly shows the existence of an ILR and, to our knowledge, this is the first time it has been clearly shown using stellar kinematics. In the only other known example, Teuben et al. (1986) showed this using gas kinematics in the strongly barred galaxy NGC 1365. Our result also gives an estimate of the ILR location, which provides useful constraints for future dynamical studies of M31 since it could be used to set limits to the bar pattern speed. These metal-rich clusters share the population properties (metallicity and age) of the integrated light in the inner few kpc, which has been studied both via spectroscopy and via deep color–magnitude diagrams from *HST* and adaptive optics imaging. By contrast, clusters with  $[\text{Fe}/\text{H}]$  less than  $-0.6$  within 2 kpc of the major axis show little rotational support and a velocity dispersion which increases as radial distance to the center decreases.

Our data do not probe the small region (200 pc) occupied by M31’s classical bulge in the description of Beaton et al. (2007), so we cannot comment on its kinematics. However, we caution against simply interpreting a high velocity dispersion in M31’s inner few kpc as a bulge velocity dispersion and then using it

to constrain M31's black hole mass (as done most recently by Saglia et al. 2010): the contribution of the bar, which dominates the light there, needs to be assessed.

H.L.M. thanks the NSF for support under grant AST-0607518, A.J.R. for grants AST-0808099 and AST-0909237, and E.A. the ANR for ANR-06-BLAN-0172. R.P.S. is supported by Gemini Observatory, which is operated by the Association of Universities for Research in Astronomy, Inc., on behalf of the international Gemini partnership of Argentina, Australia, Brazil, Canada, Chile, the United Kingdom, and the United States of America. We also thank John Wiley and Sons for permission to reproduce Figure 2.

## REFERENCES

- Athanassoula, E. 2005, *MNRAS*, **358**, 1477
- Athanassoula, E., & Beaton, R. L. 2006, *MNRAS*, **370**, 1499
- Barmby, P., Huchra, J. P., Brodie, J. P., Forbes, D. A., Schroder, L. L., & Grillmair, C. J. 2000, *AJ*, **119**, 727
- Beasley, M. A., Brodie, J. P., Strader, J., Forbes, D. A., Proctor, R. N., Barmby, P., & Huchra, J. P. 2005, *AJ*, **129**, 1412
- Beaton, R. L., et al. 2007, *ApJ*, **658**, L91
- Binney, J., Gerhard, O., & Spergel, D. 1997, *MNRAS*, **288**, 365
- Binney, J., Gerhard, O. E., Stark, A. A., Bally, J., & Uchida, K. I. 1991, *MNRAS*, **252**, 210
- Binney, J., & Tremaine, S. 2008, *Galactic Dynamics* (Princeton, NJ: Princeton Univ. Press)
- Brinks, E., & Shane, W. W. 1984, *A&AS*, **55**, 179
- Bureau, M., & Athanassoula, E. 1999, *ApJ*, **522**, 686
- Caldwell, N., Harding, P., Morrison, H., Rose, J. A., Schiavon, R., & Kriessler, J. 2009, *AJ*, **137**, 94
- Caldwell, N., Schiavon, R., Morrison, H., Rose, J., & Harding, P. 2010, *AJ*, submitted
- Colucci, J. E., Bernstein, R. A., Cameron, S., McWilliam, A., & Cohen, J. G. 2009, *ApJ*, **704**, 385
- Davies, R. L., Efstathiou, G., Fall, S. M., Illingworth, G., & Schechter, P. L. 1983, *ApJ*, **266**, 41
- de Vaucouleurs, G. 1958, *ApJ*, **128**, 465
- Fabricant, D., et al. 2005, *PASP*, **117**, 1411
- Freedman, W. L., & Madore, B. F. 1990, *ApJ*, **365**, 186
- Huchra, J. P., Brodie, J. P., & Kent, S. M. 1991, *ApJ*, **370**, 495
- Kent, S. M. 1989, *AJ*, **97**, 1614
- Kent, S. M. 1989, *PASP*, **101**, 489
- Kormendy, J., & Kennicutt, R. C., Jr. 2004, *ARA&A*, **42**, 603
- Kuijken, K., & Merrifield, M. R. 1995, *ApJ*, **443**, L13
- Lindblad, B. 1956, *Stockholms Observatorium Annaler*, Band 19, No 2
- Minniti, D., Liebert, J., Olszewski, E. W., & White, S. D. M. 1996, *AJ*, **112**, 590
- Olsen, K. A. G., Blum, R. D., Stephens, A. W., Davidge, T. J., Massey, P., Strom, S. E., & Rigaut, F. 2006, *AJ*, **132**, 271
- Saglia, R. P., et al. 2010, *A&A*, **509**, A61
- Sarajedini, A., & Jablonka, P. 2005, *AJ*, **130**, 1627
- Stark, A. A. 1977, *ApJ*, **213**, 368
- Stark, A. A., & Binney, J. 1994, *ApJ*, **426**, L31
- Stolte, A., Ghez, A. M., Morris, M., Lu, J. R., Brandner, W., & Matthews, K. 2008, *ApJ*, **675**, 1278
- Strader, J., Brodie, J. P., Cenarro, A. J., Beasley, M. A., & Forbes, D. A. 2005, *AJ*, **130**, 1315
- Teuben, P. J., Sanders, R. H., Atherton, P. D., & van Albada, G. D. 1986, *MNRAS*, **221**, 1
- Trager, S. C., Faber, S. M., Worthey, G., & González, J. J. 2000, *AJ*, **119**, 1645
- Walterbos, R. A. M., & Kennicutt, R. C., Jr. 1988, *A&A*, **198**, 61
- Weiland, J. L., et al. 1994, *ApJ*, **425**, L81
- Zinn, R. 1985, *ApJ*, **293**, 424